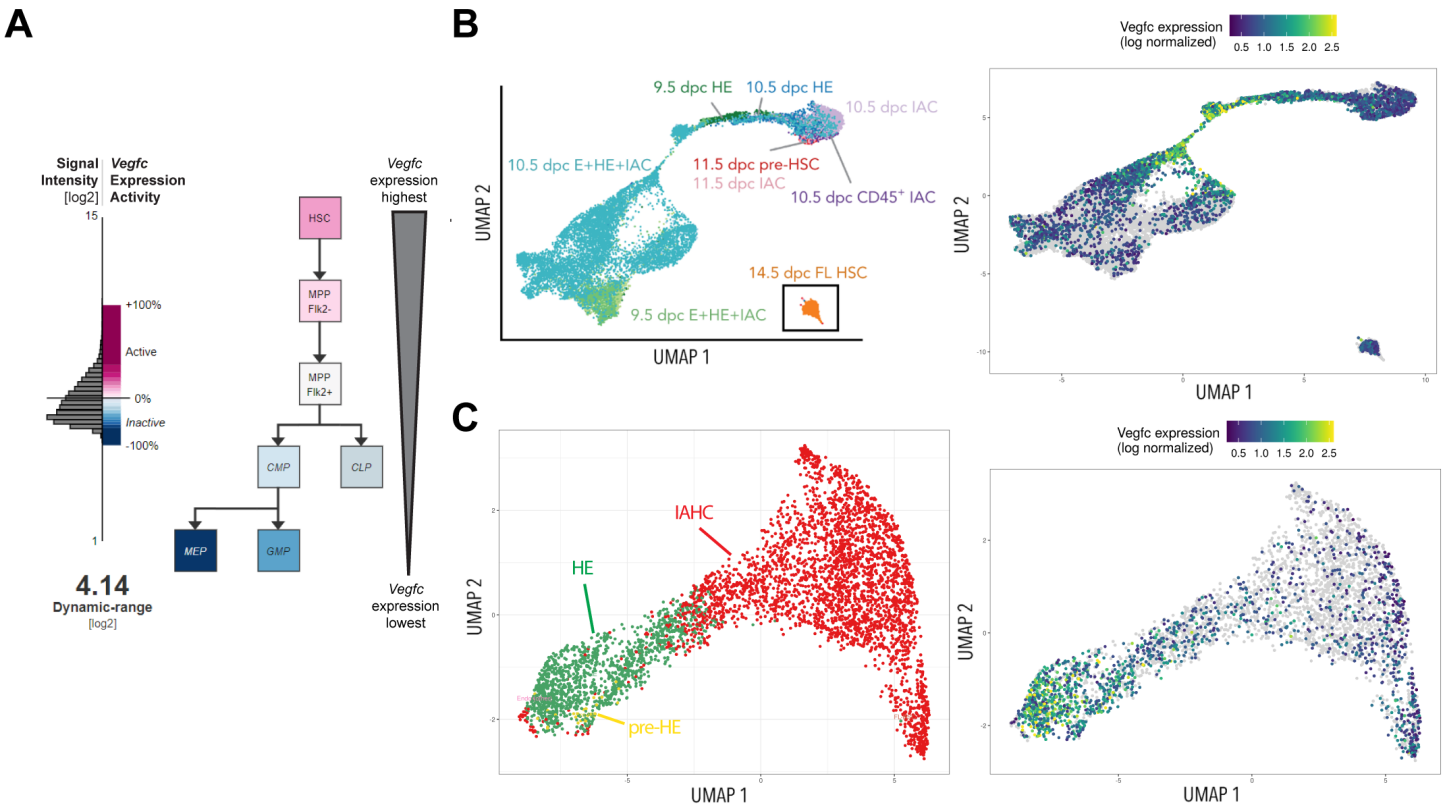

Fig. S1. Published gene expression data shows *Vegfc* is expressed in mouse HSPCs and HE.

(A) Microarray gene expression data from sorted mouse hematopoietic populations shows *Vegfc* is most highly expressed in undifferentiated HSPCs (pink) and is down-regulated in more differentiated progenitors (blue) (Seita et al., 2012, Gazit et al., 2013). (B) UMAP plot of mouse EHT using scRNA-seq data. Expression of *Vegfc* within the pre-HE and HE populations (Zhu et al., 2020). (C) Detailed UMAP of HE to intra-aortic clusters (IAC) and expression of *Vegfc* within the HE population.

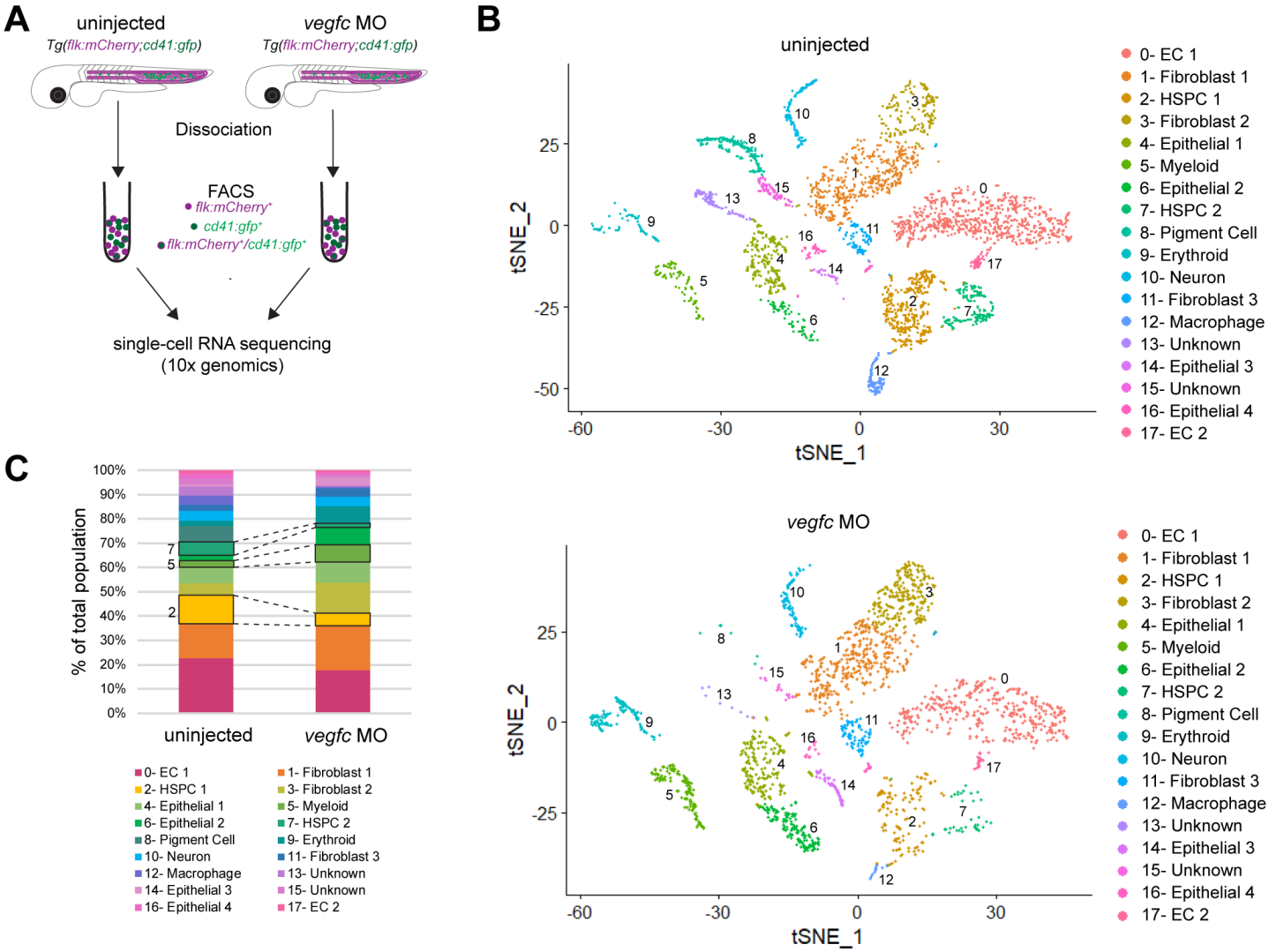

Fig. S2. Single-cell resolution map of zebrafish HSPCs and ECs at 52 hpf.

(A) Schematic of scRNA-seq experimental design. (B) t-SNE clustering map of 3,442 single cells from uninjected and 2,213 single cells from *vegfc* morphant embryos at 52 hpf. (C) Percentage of cells in each cluster (uninjected vs *vegfc* morphants (MO)). Dotted lines depict cluster size changes of interest. Raw and processed scRNA-seq data has been deposited in the NCBI GEO database (GSE186565).

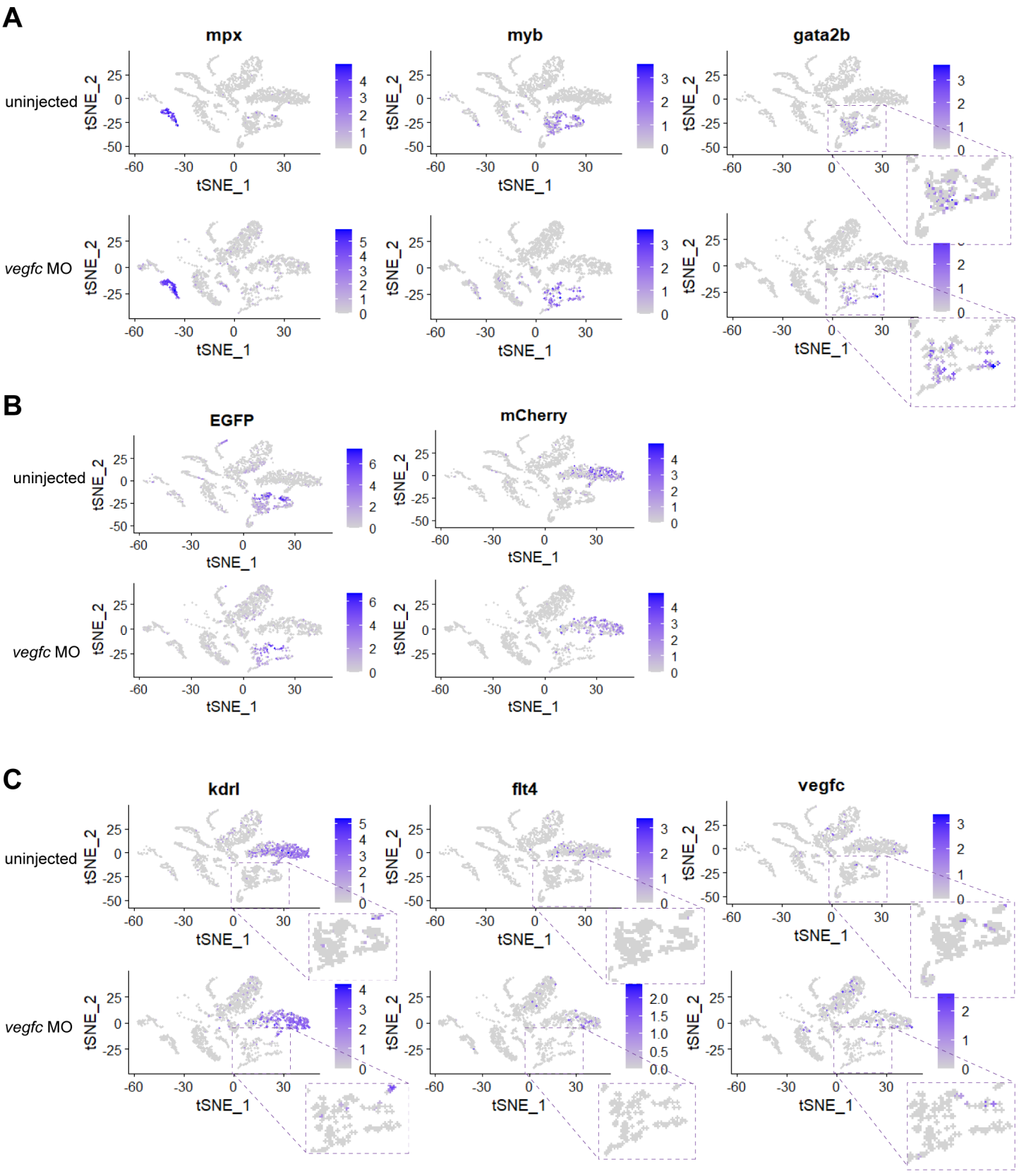

Fig. S3. scRNA-seq of HSPCs and ECs at 52 hpf shows *vegfc* and its receptors are expressed.

Comparison of marker expression in scRNA-seq datasets from uninjected controls and *vegfc* morphants (MO). (A) Identification of hematopoietic populations using known genetic markers: myeloid cells (*mpx*); HSPCs (*myb*, *gata2b*). (B) Confirmation of HSPC and EC clusters using expression of transgenic lines *cd41:gfp* and *flk:mCherry*. (C) Expression of *vegfc* and its receptors *kdrl (vegfr2a)* and *flt4 (vegfr3)*.

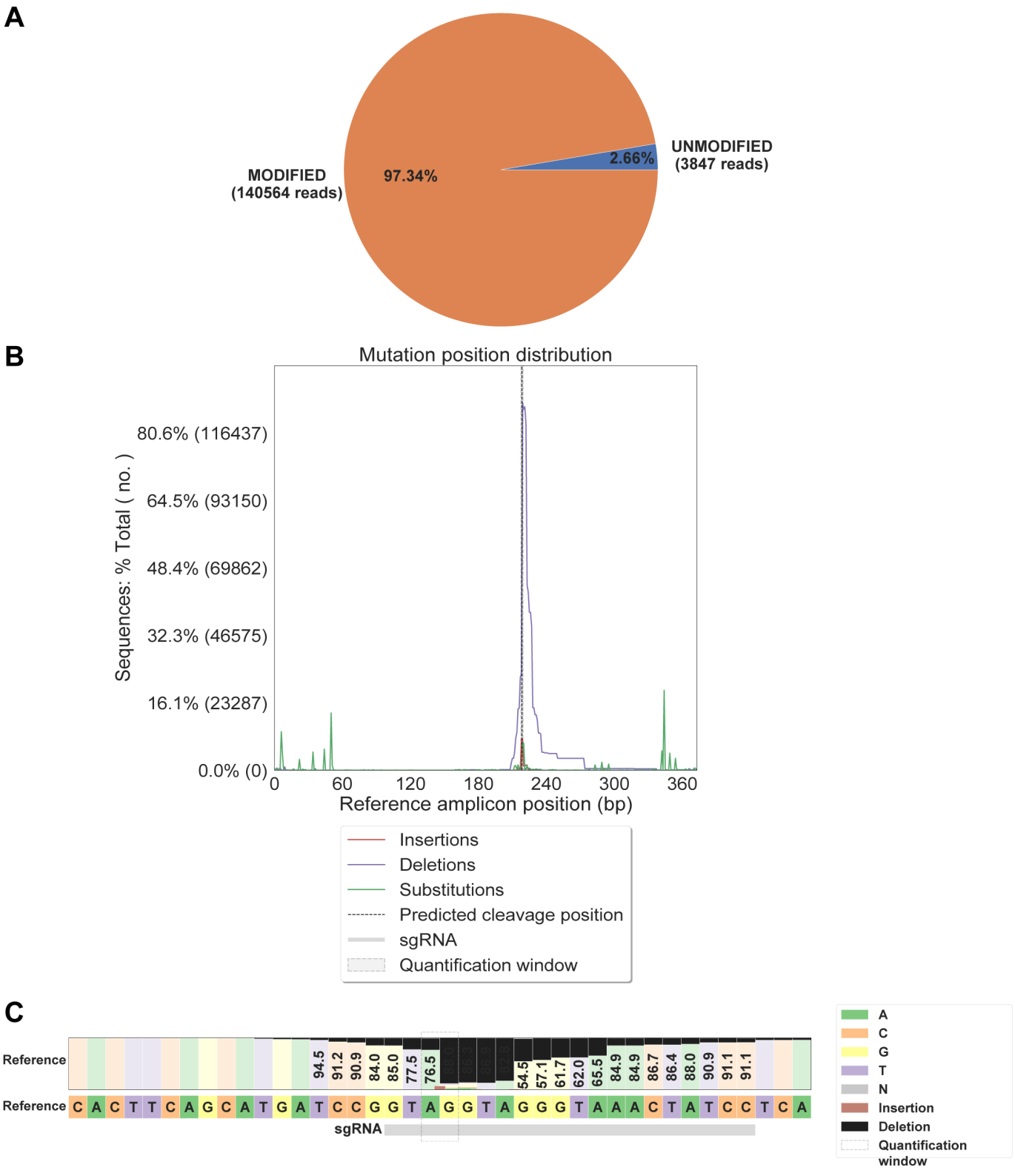

Fig. S4. Efficiency of *vegfc* sgRNA-Cas9 ribonucleoprotein complex (RNP) in pooled F0 embryos.

Genomic DNA was extracted from a minimum of 15 embryos injected with *vegfc* sgRNA-Cas9 RNP (Burger et al., 2016), followed by Illumina MiSeq sequencing and CRISPResso2 analysis (Clement et al., 2019). (A) Alignment and editing frequency of reads as determined by the percentage and number of sequence reads showing modified alleles. Our *vegfc* sgRNA sequence shows a 97.34% modification rate. (B) Frequency of insertions (red), deletions (purple), and substitutions (green) across the amplicon. *vegfc* sgRNA sequence showed high rate of deletion around the quantification window. (C) Nucleotide distribution around the *vegfc* sgRNA sequence: GTAGGTAGGGTAAACTATCC

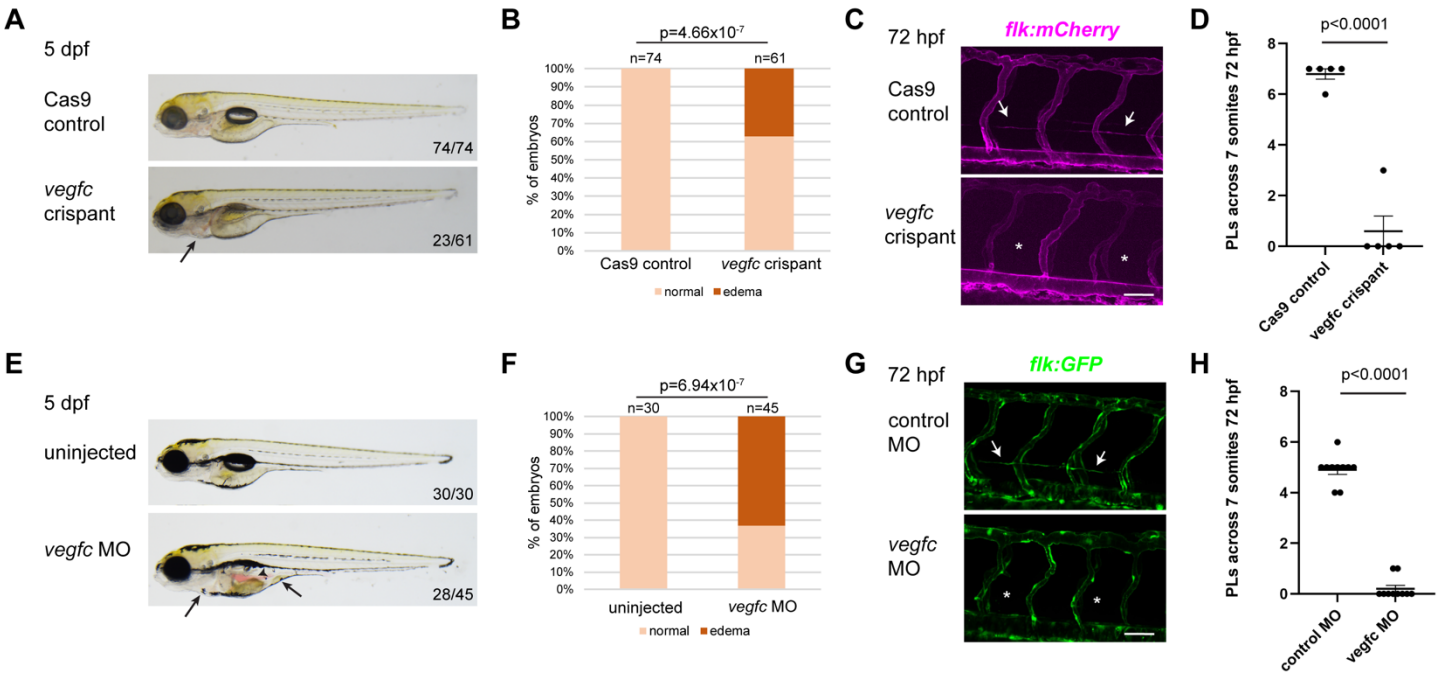

Fig. S5. *vegfc* crispants and morphants phenocopy lymphatic defects in *vegfc* mutants.

(A) Representative images of 5 dpf Cas9 control and *vegfc* crispant embryos. The black arrow indicates area of cardiac edema. All control embryos displayed normal morphology (73/73), whereas *vegfc* crispants exhibited edema (23/61). (B) Quantification of embryos shows a significant number of *vegfc* crispants have edema ($p=4.66x10^{-7}$; chi-square goodness of fit test). (C) Parachordal lymphangioblasts (PLs) are absent from the horizontal myoseptum in *flk:mCherry* (magenta) *vegfc* crispants (asterisk), as compared with Cas9 control-injected siblings at 72 hpf (arrows indicate PLs). (D) Quantification of PLs counted across 7 somites at 72 hpf in control (n=5) and *vegfc* crispant (n=5) embryos. PLs are significantly reduced in *vegfc* crispants ($p<0.0001$; unpaired two-tailed t-test). (E) Representative images of 5 dpf uninjected and *vegfc* morphant embryos. The anterior black arrow indicates an area of cardiac edema, and the posterior black arrow indicates gut edema. The black arrowhead indicates blood pooling. All uninjected embryos (30/30) in this experiment, and previously injected control morphants (data not shown), displayed normal morphology at 5 dpf. Conversely, vegfc morphants exhibited edema and blood pooling (28/45). (F) Quantification of embryos shows a significant number of *vegfc* morphants have edema ($p=6.94x10^{-7}$; chi-square goodness of fit test). (G) PLs are absent from the horizontal myoseptum in *flk:GFP* (green) *vegfc* morphants (asterisk), as compared with control morphants at 72 hpf (arrows indicate PLs). (H) Quantification of PLs counted across 7 somites at 72 hpf in control (n=10) and *vegfc* morphant (n=10) embryos. PLs are significantly reduced in *vegfc* morphants ($p<0.0001$; unpaired two-tailed t-test). Error bars show mean ± SEM. Scale bars: 50 μm (C,G).

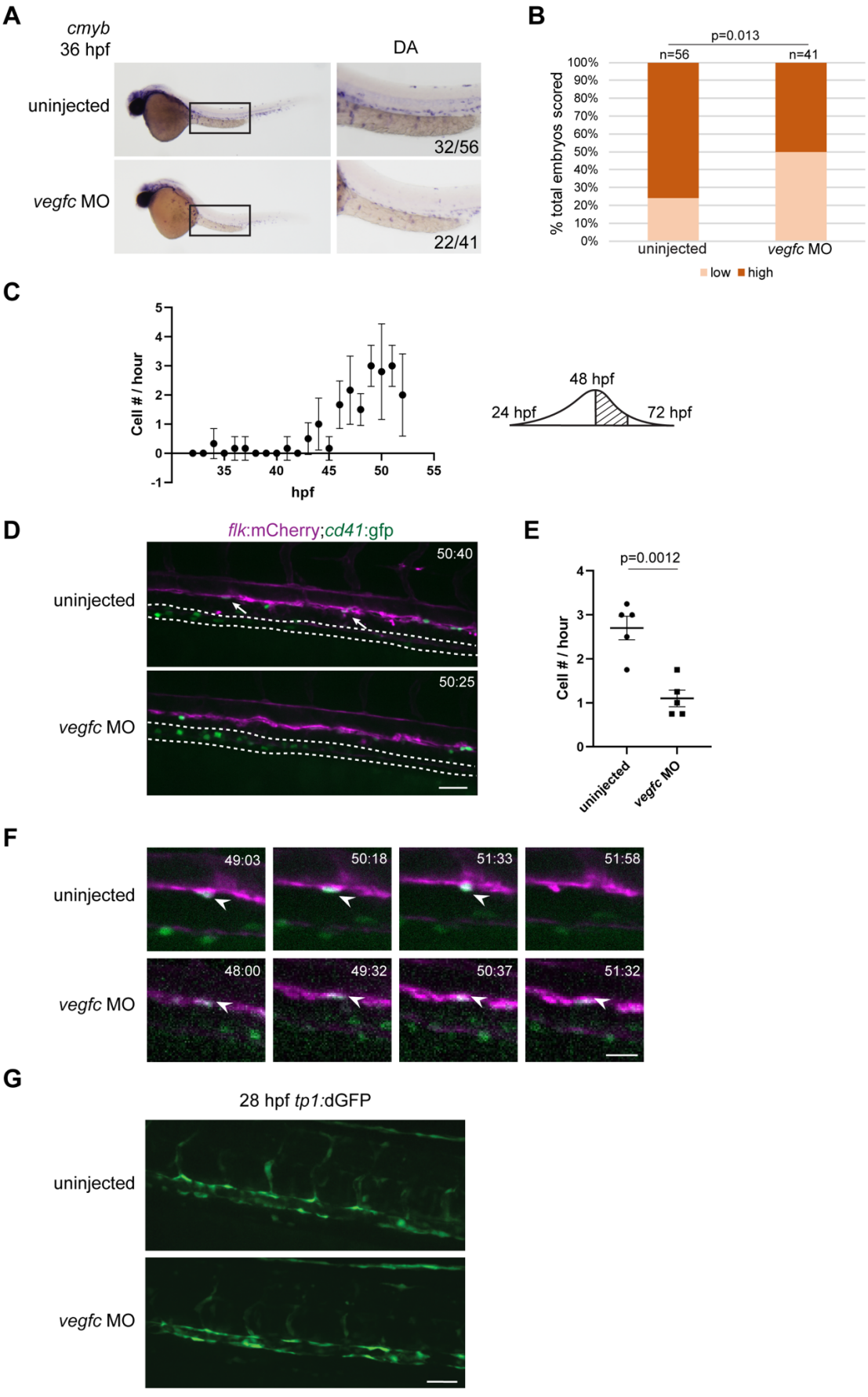

Fig. S6. *vegfc* morphants have decreased HSPC emergence from the DA.

(A) *cmyb* expression in the DA at 36 hpf in *vegfc* morphants (MO) and uninjected controls. (B) Percentage of embryos scored and classified as having low or high *cmyb* expression (p=0.013; chi-square goodness of fit test).

(C) Quantification of *cd41:gfp*+ HSPC emergence (Cell number (#) / hour) from *flk:mCherry*+ HE (32-52 hpf; n=12 embryos). Schematic showing the wave of emergence from the DA. (D-F) The experiment begins from the peak of emergence at 48 hpf (hatched region in (C)). (D) Single frame of time-lapse (hpf:min) showing *cd41:gfp*+ HSPCs (arrows, green) budding from *flk:mCherry*+ HE (magenta) in uninjected (top panel) or *vegfc* morphant embryos (bottom panel). White arrows indicate cells undergoing EHT. Dotted line outlines developing pronephric tubules. (E) Quantification of the total number of *cd41:gfp*+ HSPCs budding from the DA between 48 and 52 hpf, divided by 4 to give cell number (#) / hour (p=0.0012; unpaired two-tailed t-test). (F) 4 frames selected from uninjected and *vegfc* morphant time-lapse movies depicting HSPC budding (top panels) and static hammock cell (bottom panels). White arrowheads indicate the cell of interest. (G) Specification of the DA and notch activity is unchanged in *vegfc* morphant embryos. Representative images of *tp1:dGFP* (green) expression in uninjected and *vegfc* morphant embryos at 28 hpf (n=8 embryos per treatment group). Error bars show mean ± SEM. Scale bars: 50 μm (D,G); 10 μm (F).

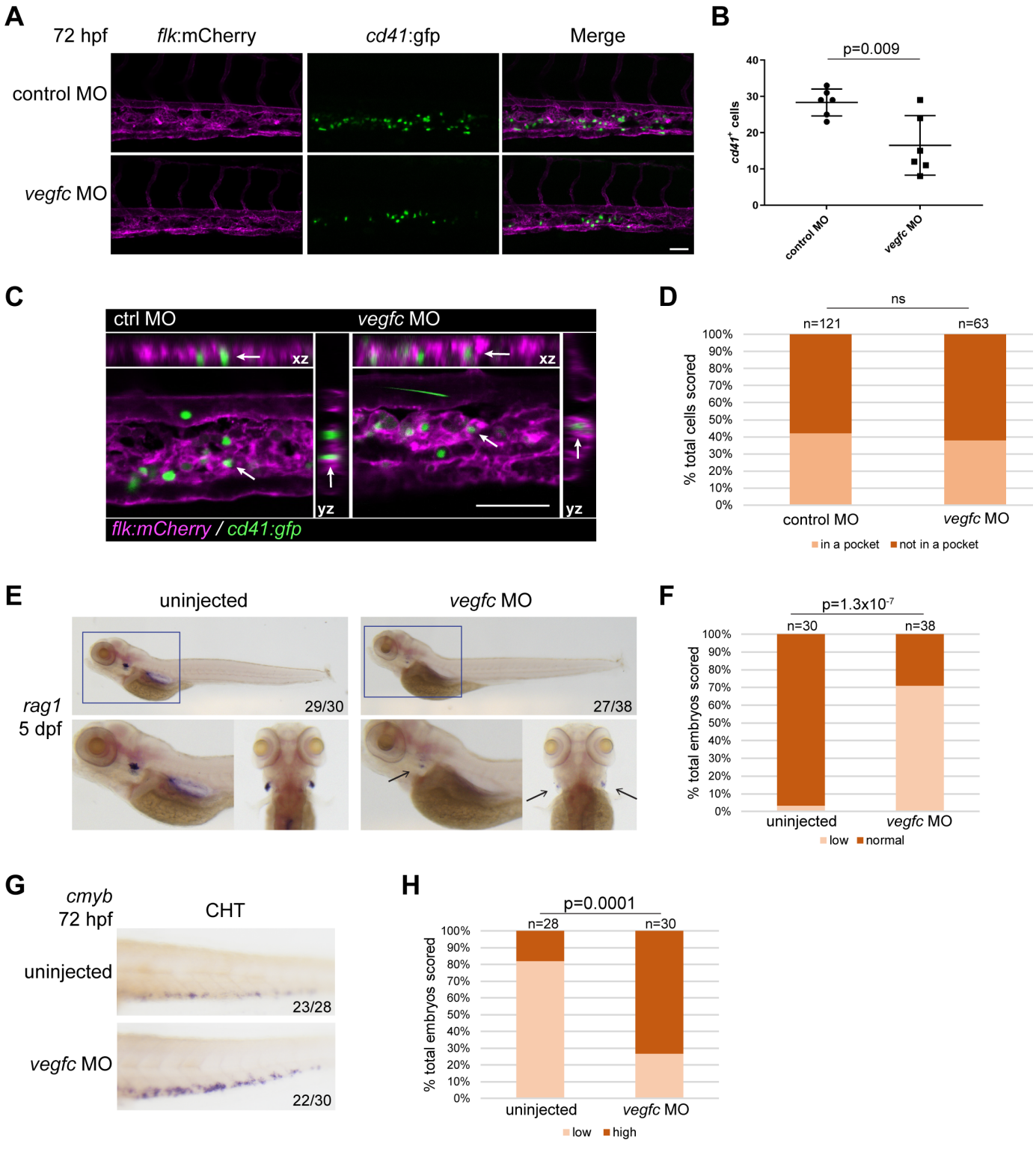

Fig. S7. *vegfc* loss-of-function leads to altered definitive hematopoiesis throughout development.

(A) *In vivo* imaging of *cd41:gfp* (green) / *flk:mCherry* (magenta) depicting decreased HSPC numbers in the CHT of *vegfc* morphants (MO) at 72 hpf. (B) Quantification of *cd41:gfp*$^{+}$ cells within the CHT, as shown in (A); control versus *vegfc* morphants (p=0.0093; unpaired two-tailed t-test). (C) Representative images of *cd41:gfp/flk:mCherry* embryos in xy, xz, yz planes showing HSPCs surrounded by ECs in the CHT at 72 hpf of control and *vegfc* morphant embryos. CHT remodeling is not impaired in *vegfc* morphants. (D) There is no significant difference (ns) in the percentage of individual *cd41:gfp*+ cells within a *flk:mCherry*+ EC pocket between control embryos (n=121) or *vegfc* morphants (n=63). (E) *vegfc* morphants show decreased *rag1* expression in the thymus at 5 dpf. Black arrow highlights area of *rag1* staining in *vegfc* morphant. (F) Percentage of total embryos scored, classified as having low or normal *rag1* expression ($p=1.3x10^{-7}$; chi-square goodness

of fit test). (G) *vegfc* loss-of-function increases the percentage of embryos with high *cmyb* expression compared to uninjected embryos. *cmyb* expression was scored in the CHT at 72 hpf. (H) Percentage of total embryos scored and classified as having low or high *cmyb* expression (p=0.0001; chi-square goodness of fit test). Error bars show mean ± SEM. Scale bars: 40 μm (A,C).

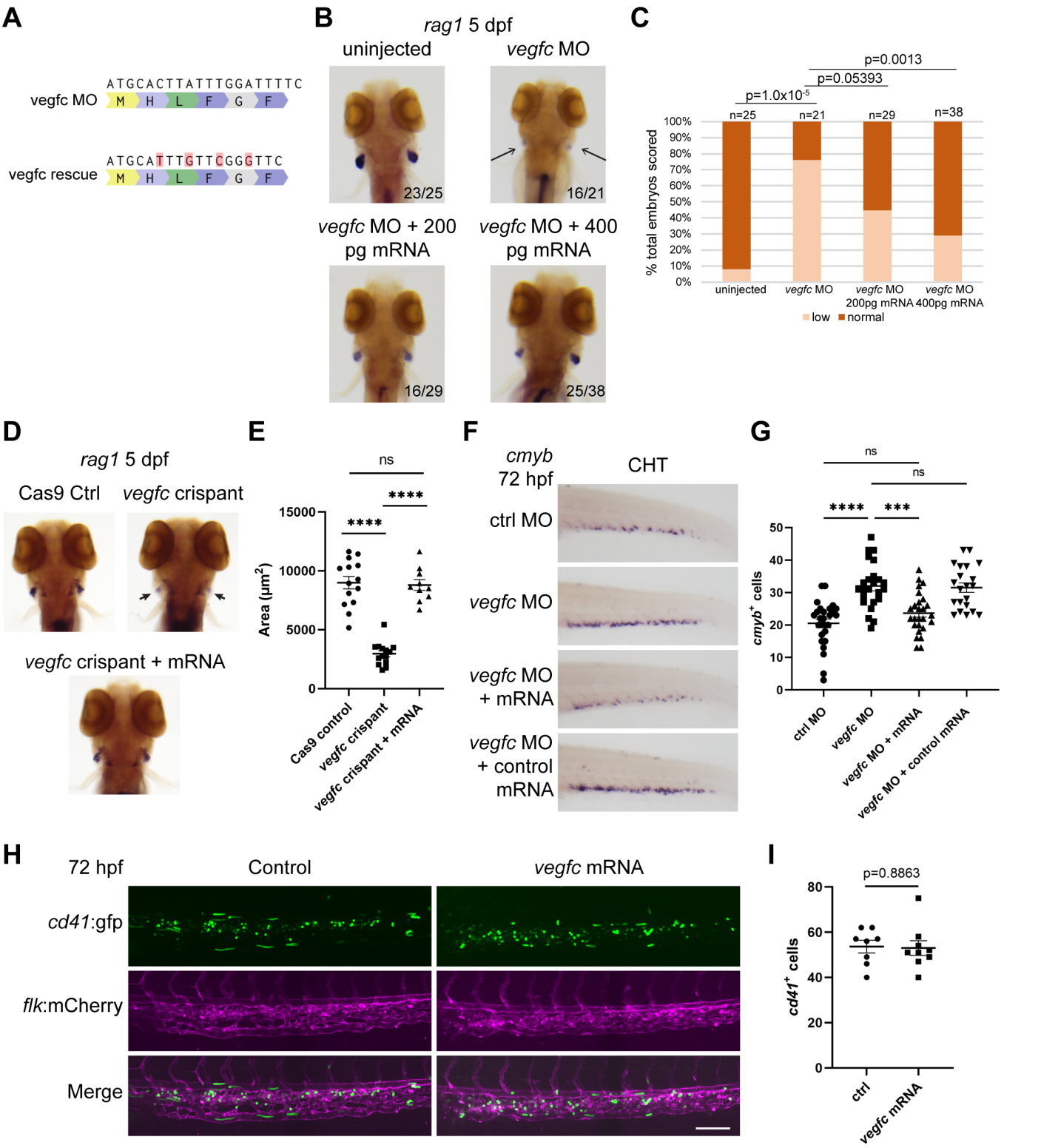

Fig. S8. Morpholino resistant *vegfc* mRNA rescues impaired definitive hematopoiesis.

(A) Schematic showing the *vegfc* morpholino (MO) target sequence with corresponding amino acids and the MO-resistant rescue mRNA with altered base pairs highlighted in red. Corresponding amino acid sequence remains the same as endogenous vegfc. (B) *vegfc* morphants show decreased *rag1* expression in the thymus at 5 dpf. Injection of 200 pg rescue mRNA trends toward restoring the level of *rag1* expression. Injection of 400 pg rescue mRNA restores significant *rag1* expression, as compared to *vegfc* morphant embryos. Black arrow highlights area of *rag1* staining in *vegfc* morphant. (C) Percentage of total embryos scored, classified as having low or normal *rag1* expression (uninjected vs *vegfc* MO, $p=1.0\times10^{-5}$; *vegfc* MO vs *vegfc* MO + 200pg mRNA, p=0.05393; *vegfc* MO vs *vegfc* MO + 400pg mRNA, p=0.0013; chi-square goodness of fit test). (D) *vegfc*

crispants show decreased *rag1* expression in the thymus at 5 dpf. Injection of 400 pg rescue restores significant *rag1* expression, as compared to *vegfc* crispant treated embryos. Black arrow highlights area of *rag1* staining in *vegfc* crispant. (E) Quantification of the area of *rag1* expression: Cas9 control vs *vegfc* crispant, ****p<0.0001; *vegfc* crispant vs *vegfc* crispant + 400pg rescue mRNA, ****p<0.0001; Cas9 control vs *vegfc* crispant + 400pg rescue mRNA, not significant (one-way ANOVA). (F) *vegfc* morphants show increased *cmyb* expression compared to control MO. Co-injection of *vegfc* MO and 400 pg rescue mRNA restores *cmyb* expression to control levels. In contrast, co-injection of *vegfc* MO and 400 pg control mRNA does not restore *cmyb* expression. (G) Quantification of *cmyb*$^{+}$ cells in the CHT: control MO vs *vegfc* MO, ****p<0.0001; *vegfc* MO vs *vegfc* MO + 400pg rescue mRNA, ***p=0.0002; *vegfc* MO vs *vegfc* MO + 400pg control mRNA, not significant; control MO vs *vegfc* MO + 400pg rescue mRNA, not significant (one-way ANOVA). (H) Overexpression of *vegfc* in a *cd41:gfp* (HSPCs; green) / *flk:mCherry* (blood vessels; magenta) background using MO-resistant mRNA. (I) Quantification of *cd41:gfp*$^{+}$ cells in the CHT at 72 hpf (p=0.8863; unpaired two-tailed t-test). Error bars show mean ± SEM. Scale bar: 50 μm (H).

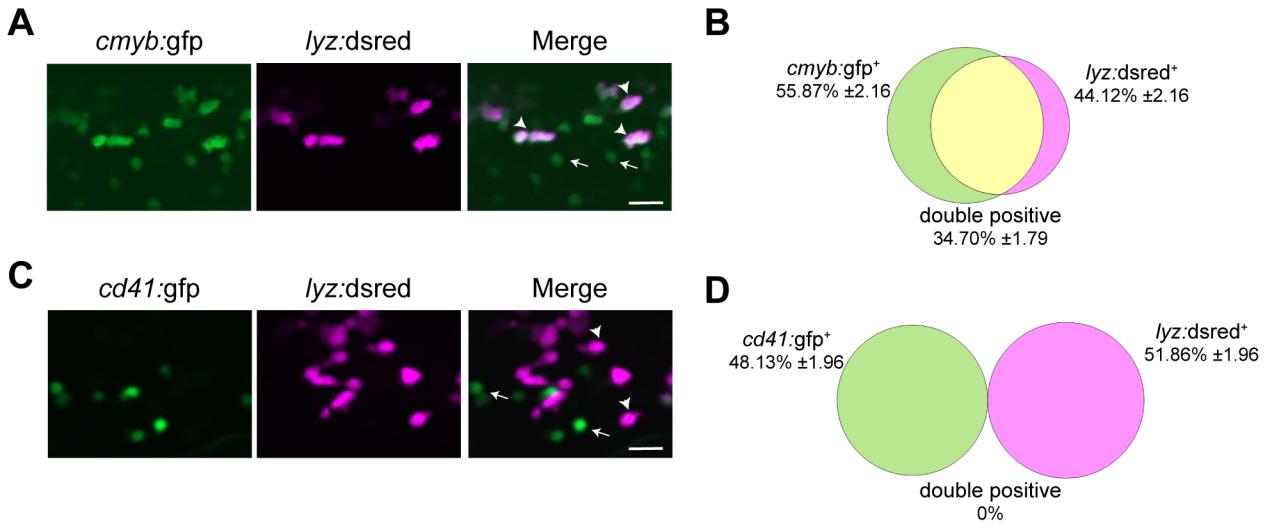

Fig. S9. *cmyb:gfp* marks myeloid cells in addition to HSPCs but *cd41:gfp* does not.

(A) A large number of *cmyb:gfp*+ (green) cells co-localize with neutrophil marker *lyz:DsRed2*$^{+}$ (magenta) cells at 72 hpf. Arrowheads indicate cells positive for *cmyb:gfp* and *lyz:DsRed2*, arrows indicate cells positive for *cmyb:gfp* but not *lyz:DsRed2*. (B) Quantification of the percentage of cells positive for *cmyb:gfp*, *lyz:DsRed2,* or both (n=10 embryos). (C) There were no signs of co-localization between *cd41:gfp*+ (green) cells and *lyz:DsRed2*+ (magenta) cells at 72 hpf. Arrowheads indicate cells positive for *lyz:DsRed2*, arrows indicate cells positive for *cd41:gfp*. (D) Quantification of the percentage of cells positive for *cd41:gfp*, *lyz:DsRed2,* or both (n=8 embryos). Error bars show mean ± SEM. Scale bars: 20 μm (A,C).

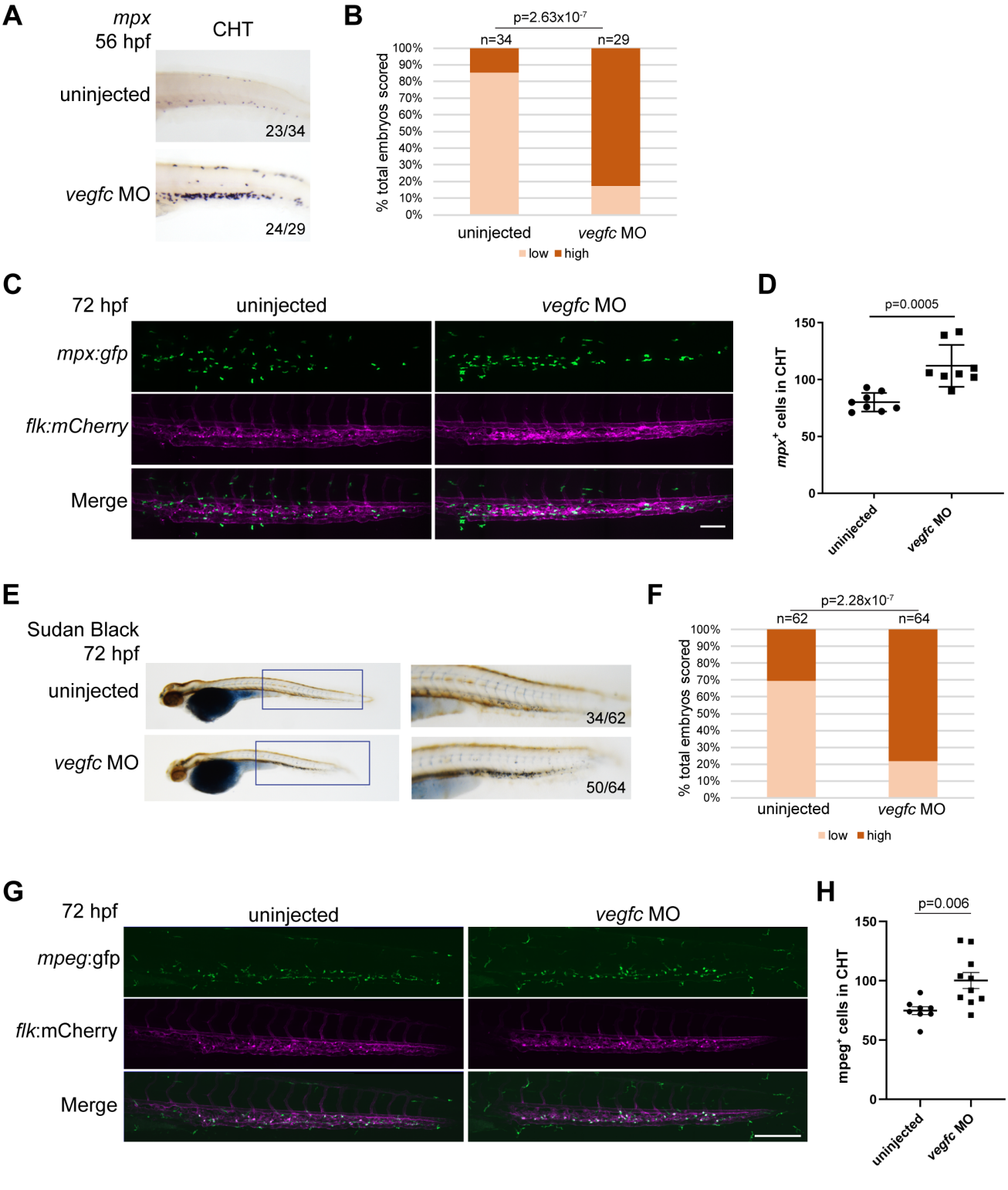

Fig. S10. Neutrophil and macrophage numbers are increased in the CHT of *vegfc* morphant embryos.

A) *vegfc* morphants (MO) have higher *mpx* expression in the CHT region at 56 hpf. (B) Percentage of total embryos scored, classified as having low or high *mpx* expression ($p=2.63x10^{-7}$; chi-square goodness of fit test). (C) *vegfc* morphants have more *mpx:gfp*+ (green) cells in the CHT at 56 hpf. Blood vessels are shown by *flk:mCherry* (magenta). (D) Quantification of *mpx:gfp*+ cells within the CHT (p=0.0005; unpaired two-tailed t-test). (E) *vegfc* morphants have increased neutrophils as shown by Sudan black staining at 72 hpf. (F) Percentage of embryos scored, classified as having low or high levels of Sudan black staining ($p=2.28x10^{-7}$; chi-square goodness of fit test). (G) *vegfc* morphants show increased numbers of macrophages in the CHT as shown by *mpeg:gfp*+ (green) cells at 72 hpf. Blood vessels are shown by *flk:mCherry* (magenta). (H) Quantification of the number of *mpeg:gfp*+ cells within the CHT (p=0.006; unpaired two-tailed t-test). Error bars show mean ± SEM. Scale bars: (C) 50 μm; (G) 100 μm.

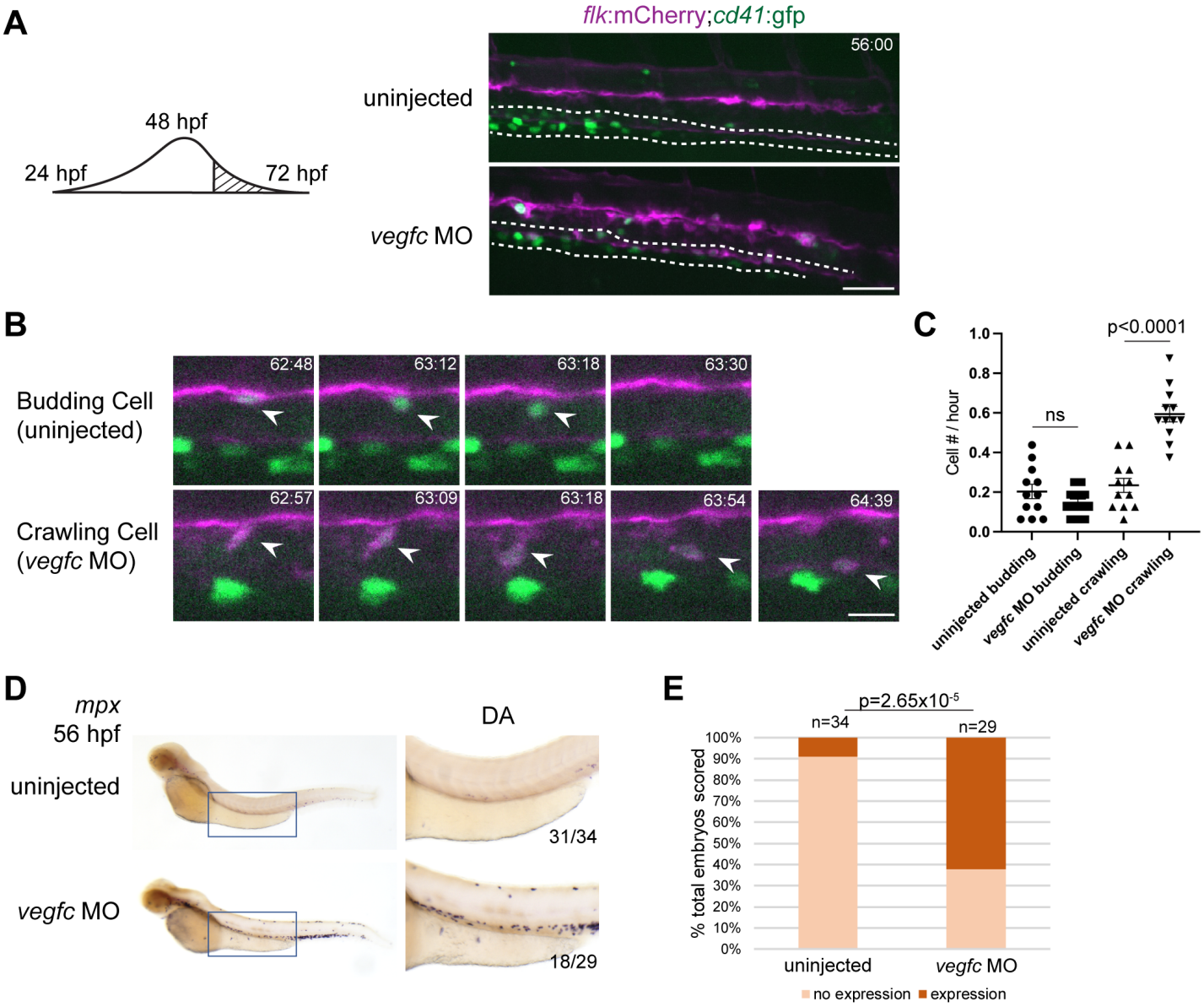

Fig. S11. Late-stage hemogenic endothelium gives rise to increased crawling myeloid-like cells in *vegfc* morphant embryos.

(A) Left: schematic showing time-lapse imaging was performed after the peak of HSPC emergence form the DA. Right: single frames of time-lapse (hpf:min) showing the overall difference in DA morphology between uninjected controls (top panel) and *vegfc* morphants (MO; bottom panel) in a *cd41:gfp* (HSPCs; green) / *flk:mCherry* (blood vessels; magenta) background. The dotted line outlines the pronephric tubules. (B) Upper: 4 frames selected from a uninjected control time-lapse movie between 56-72 depicting HSPC budding. Lower: 5 frames selected from a *vegfc* morphant time-lapse movie depicting HSPC crawling. White arrowheads indicate the cell of interest. (C) Quantification of *flk:mCherry+/cd41:gfp+* cell behavior within the DA ($p<0.0001$; one-way ANOVA). The total number of events observed are divided by the duration of the experiment (16 hours) to give the number of events per hour. The data shown is combined from two independent experiments with a total of n=12 uninjected and n=12 *vegfc* morphant embryos. (D) *vegfc* loss-of-function increases the percentage of embryos displaying high *mpx* expression in the DA region at 56 hpf. (E) Percentage of embryos scored classified as having *mpx* expression in the DA or not ($p=2.65x10^{-5}$; chi-square goodness of fit test). Error bars show mean ± SEM. Scale bars: 40 μm (A); 10 μm (B).

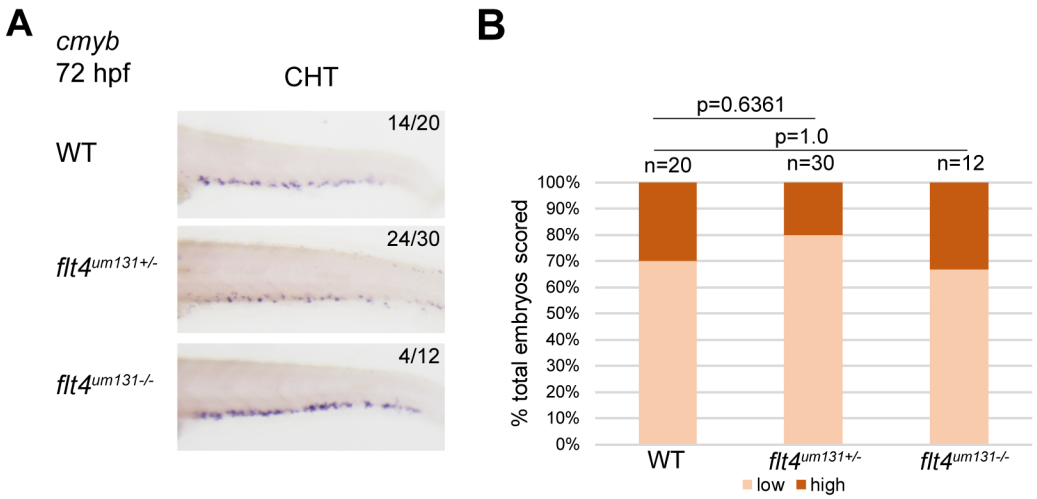

Fig. S12. *flt4 (vegfr3)* mutants have no significant change in *cmyb* expression in the CHT at 72 hpf. Compared to *vegfc*$^{um18-/-}$ mutant embryos that have increased *cmyb* expression in the CHT at 72 hpf (see Fig. 2G,H), (A) *flt4*$^{um131+/-}$ and *flt4*$^{um131-/-}$ mutant embryos show no change in *cmyb* expression in the CHT at 72 hpf when compared to WT. (B) Percentage of total embryos scored for level of *cmyb* expression. No significant difference observed in WT vs *flt4*$^{um131+/-}$ (p=0.6361; chi-square goodness of fit test), or WT vs *flt4*$^{um131-/-}$ (p=1.0; chi-square goodness of fit test).

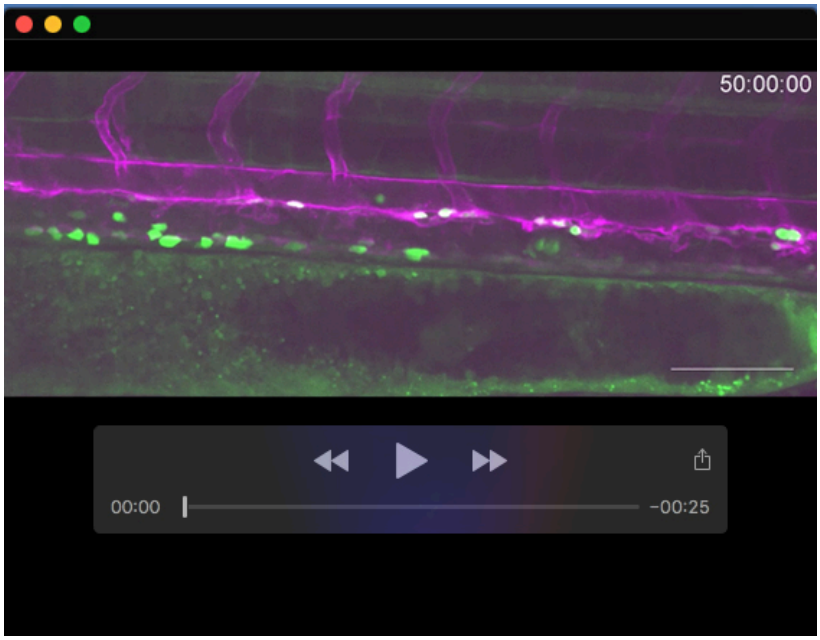

Movie 1. Control HSPC emergence from the DA.
Time-lapse imaging of *cd41:gfp* (HSPCs; green) and *flk:mCherry* (ECs; magenta) control embryos from 48-52 hpf. Arrows indicate cells that are undergoing EHT. Corresponds to Figure 1.

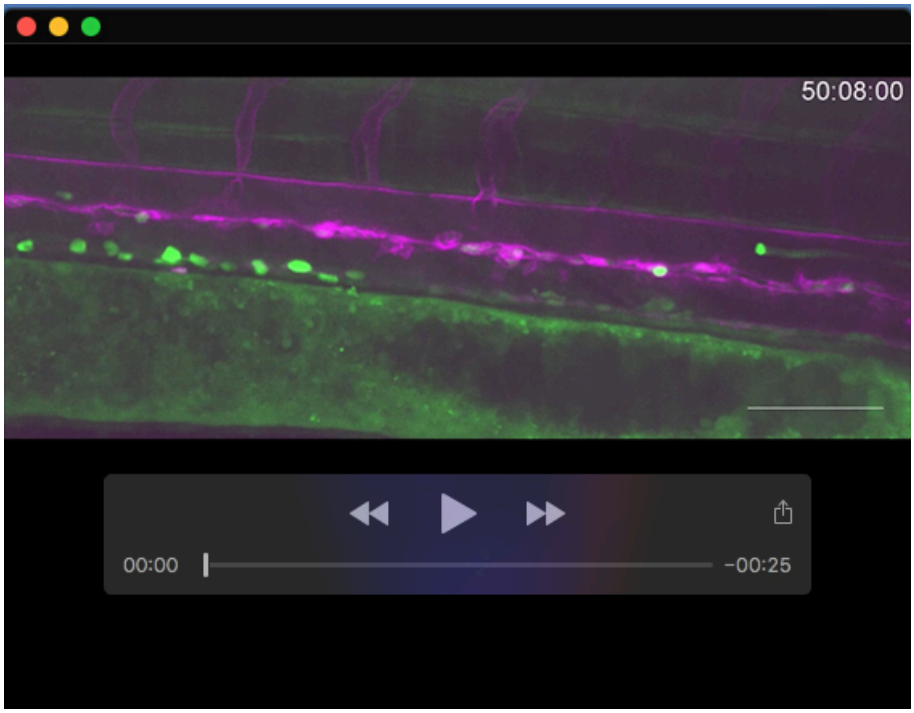

Movie 2. *vegfc* loss-of-function HSPC emergence from the DA.
Time-lapse imaging of *cd41:gfp* (HSPCs; green) and *flk:mCherry* (ECs; magenta) *vegfc* loss-of-function embryos from 48-52 hpf. Arrows indicate cells are unable to complete EHT. Corresponds to Figure 1.

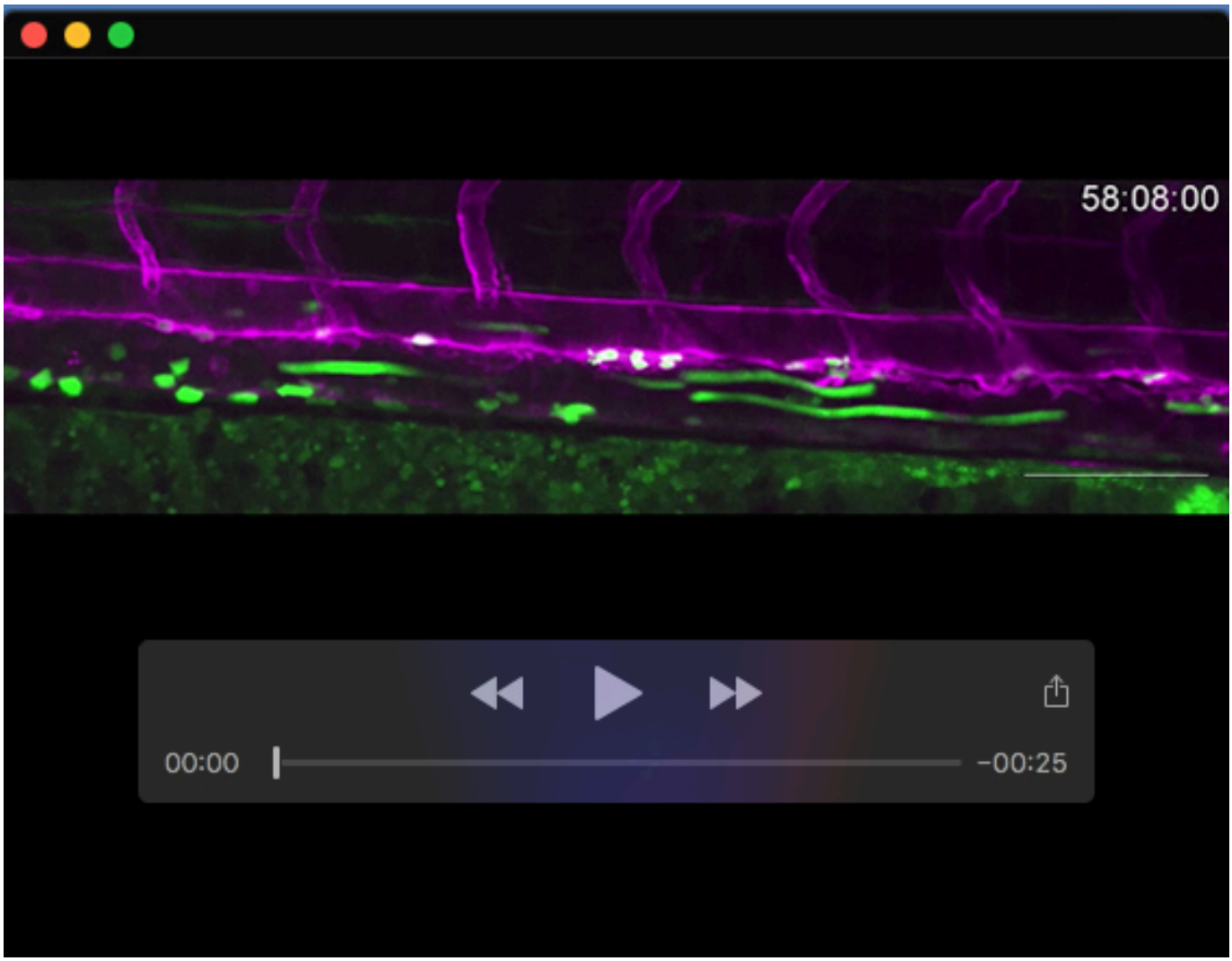

Movie 3. Control HSPC emergence from late-stage DA.
Time-lapse imaging of *cd41:gfp* (HSPCs; green) and *flk:mCherry* (ECs; magenta) control embryos from 56-72 hpf. Arrows indicate cells that are undergoing EHT. Corresponds to Figure 5A-C.

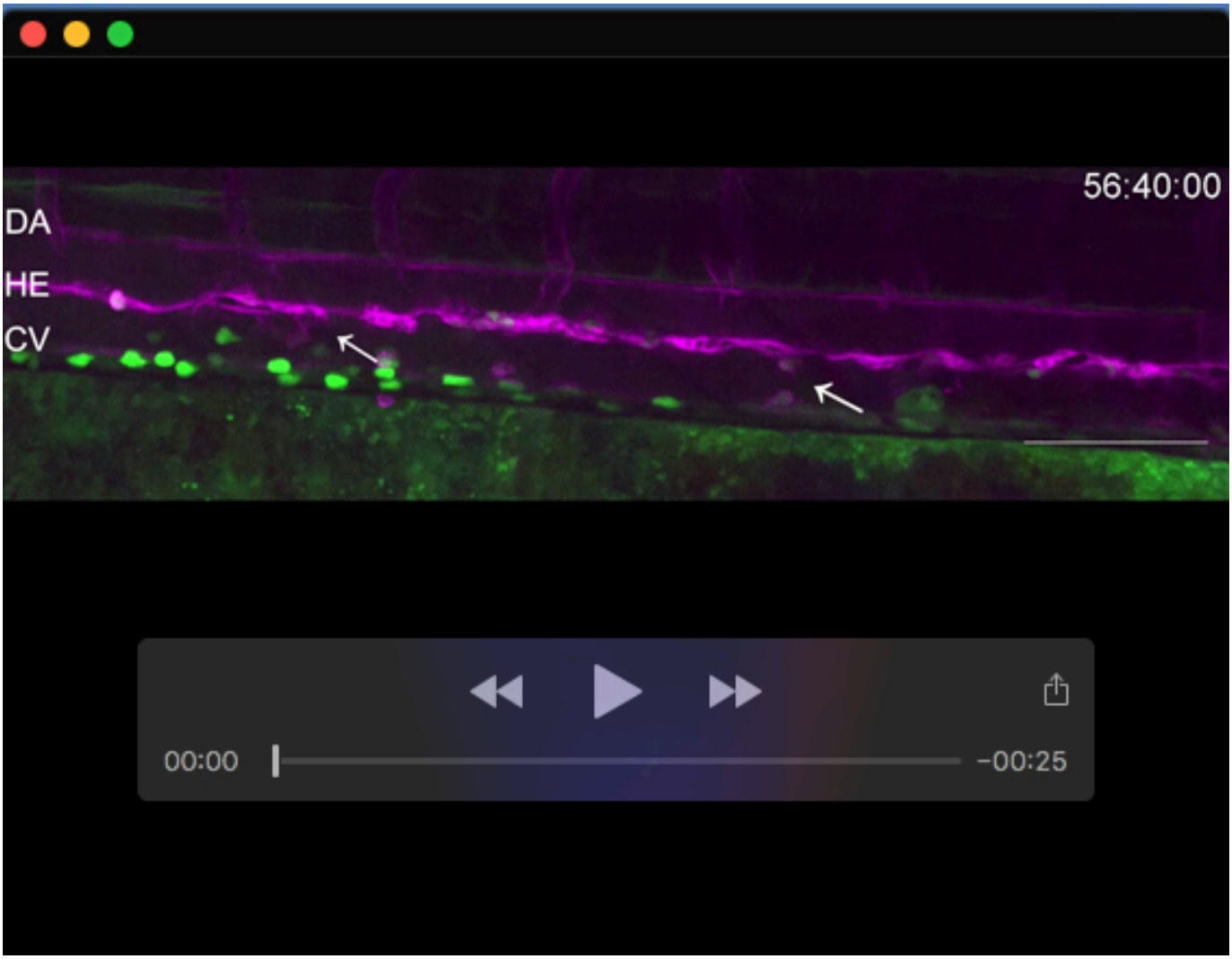

Movie 4. *vegfc* loss-of-function HSPC emergence from late-stage DA.
Time-lapse imaging of *cd41:gfp* (HSPCs; green) and *flk:mCherry* (ECs; magenta) *vegfc* loss-of-function crispant embryos from 56-72 hpf. Arrows indicate cells displaying crawling behavior. Corresponds to Figure 5A-C.

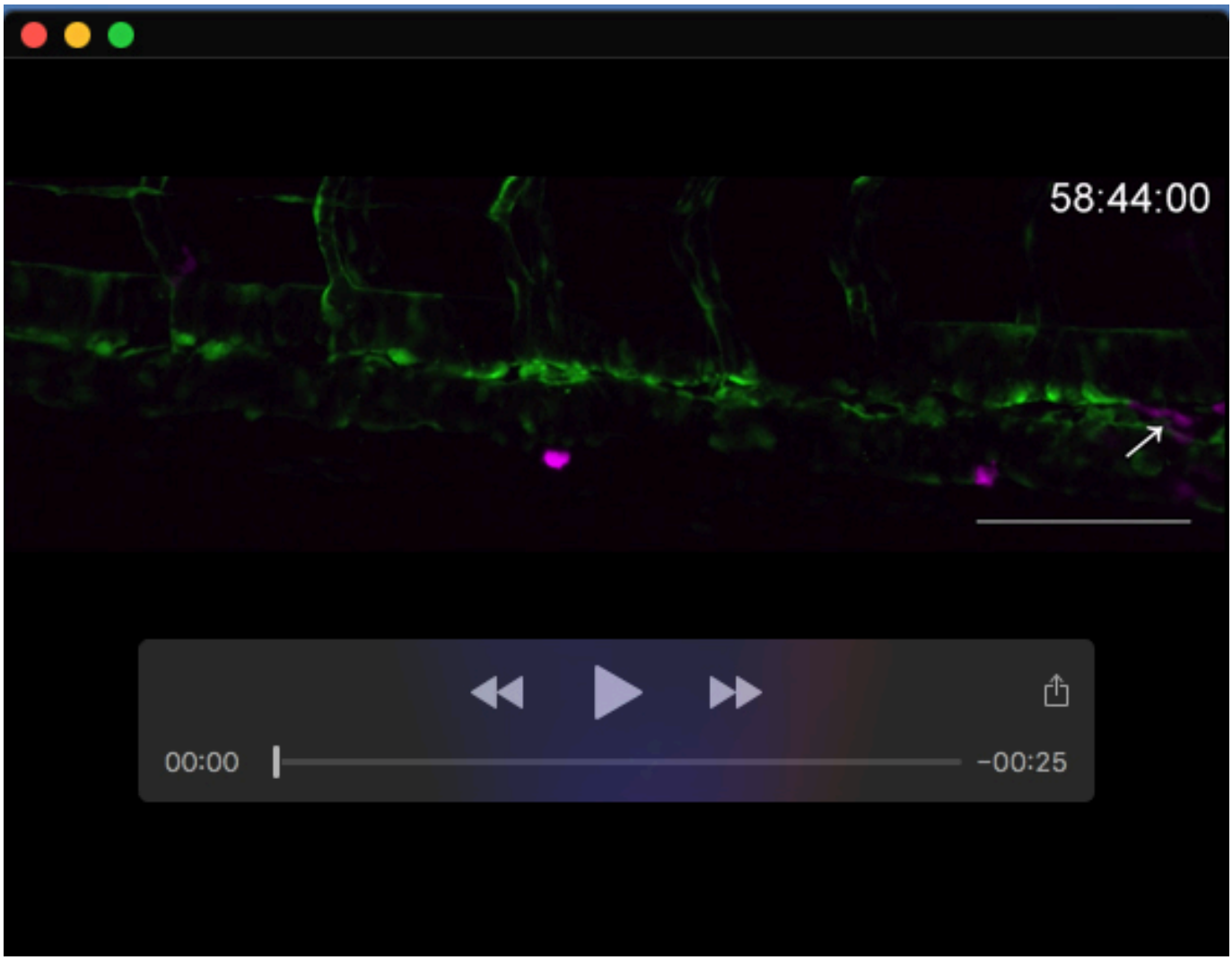

Movie 5. *lyz:DsRed2*$^{+}$ cells in control embryo late-stage DA.

Time-lapse imaging of *flk*:*gfp* (ECs; green) and *lyz:DsRed2* (myeloid; magenta) control embryos from 56-72 hpf. Arrows indicate *lyz:DsRed2*+ cells that reside in the DA and display crawling behavior. Corresponds to Figure 5D,E.

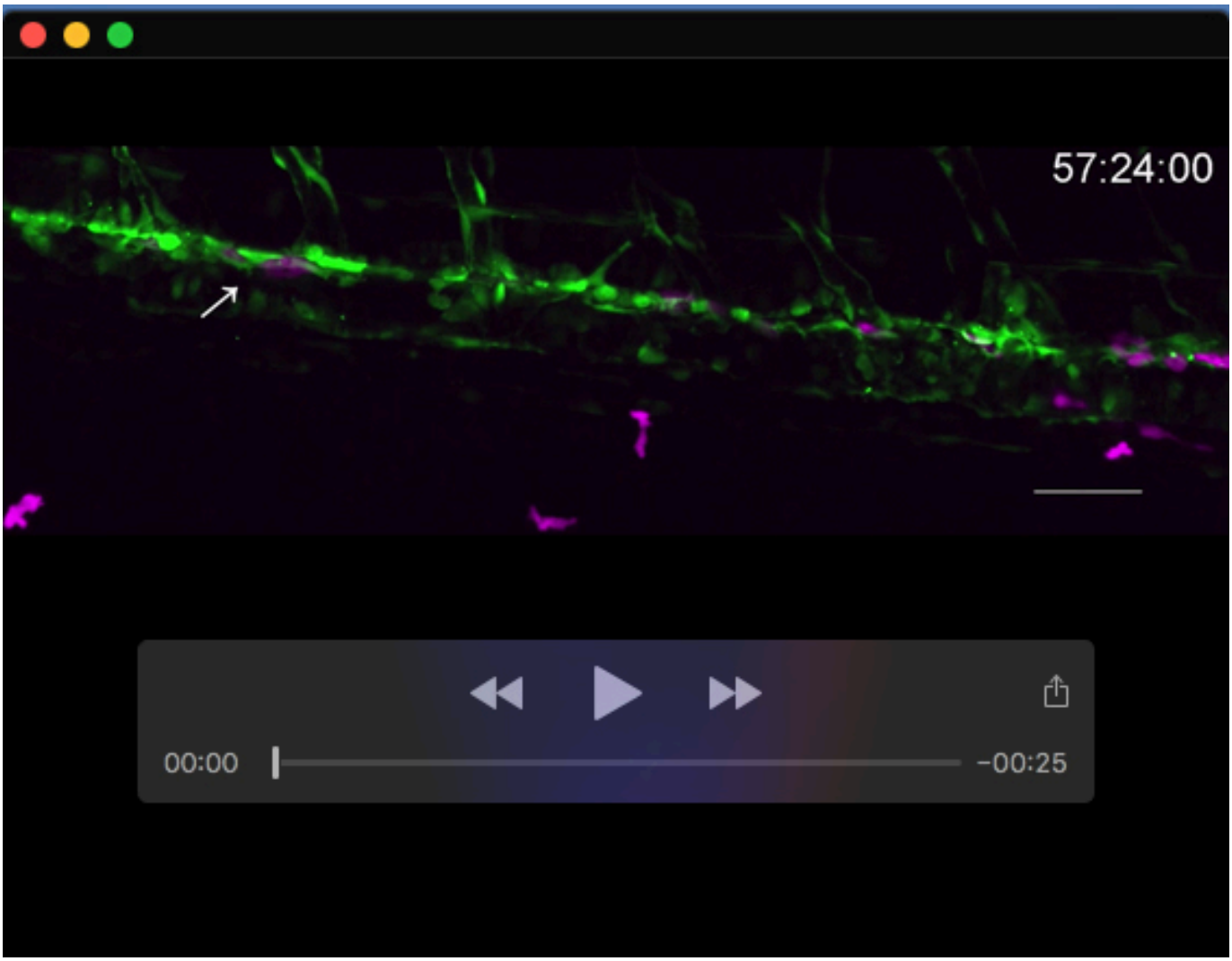

Movie 6. *lyz:DsRed2*+ cells in *vegfc* loss-of-function embryo late-stage DA.

Time-lapse imaging of *flk*:*gfp* (ECs; green) and *lyz:DsRed2* (myeloid; magenta) *vegfc* loss-of-function embryos from 56-72 hpf. Arrows indicate *lyz:DsRed2*+ cells that reside in the DA and display crawling behavior. Corresponds to Figure 5D,E.

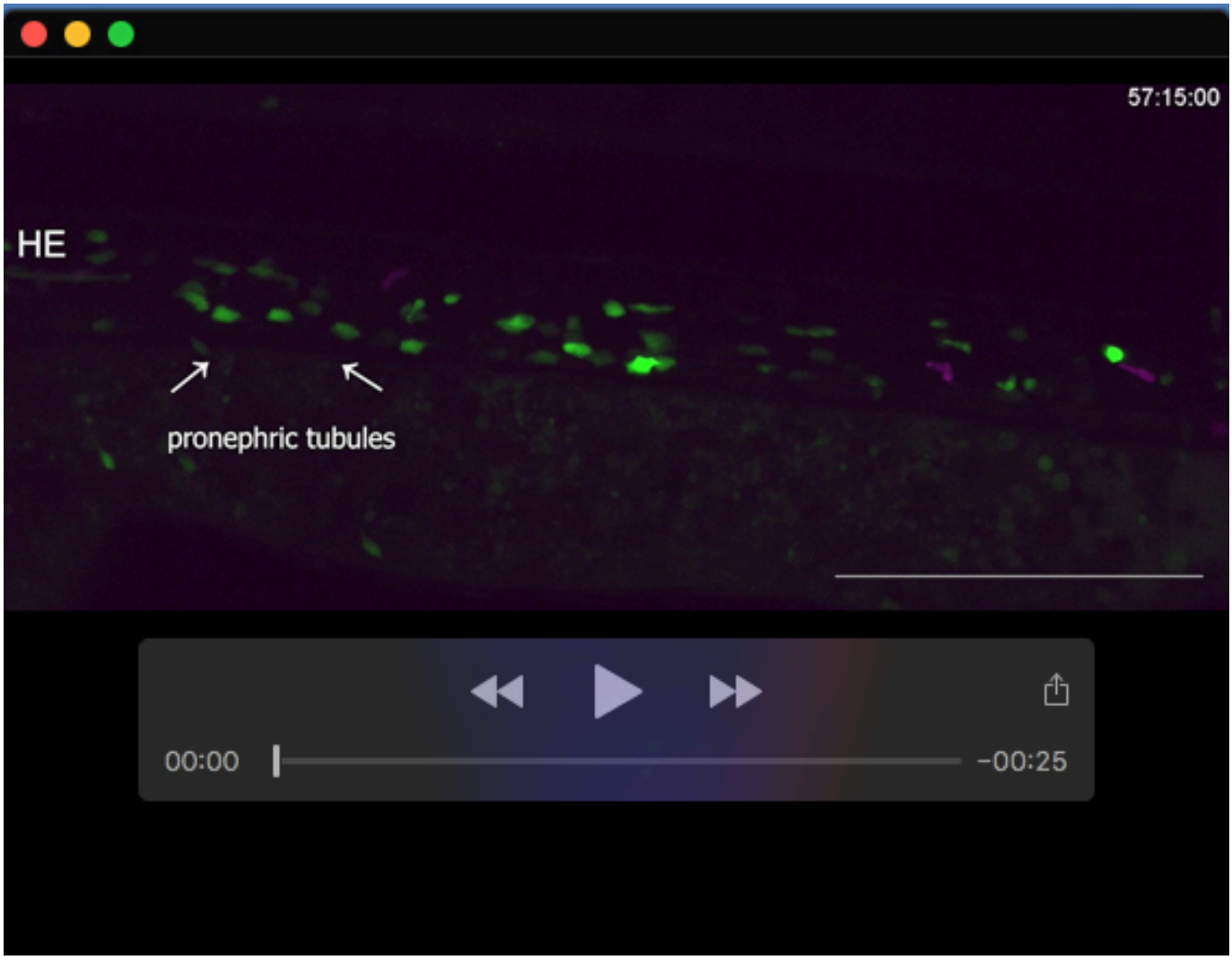

Movie 7. *lyz:DsRed2+/cd41:gfp+* cells in control embryo late-stage DA.
Time-lapse imaging of *cd41:gfp* (HSPCs; green) and *lyz:DsRed2* (myeloid; magenta) control embryos from 56- 66 hpf. Corresponds to Figure 5F,G.

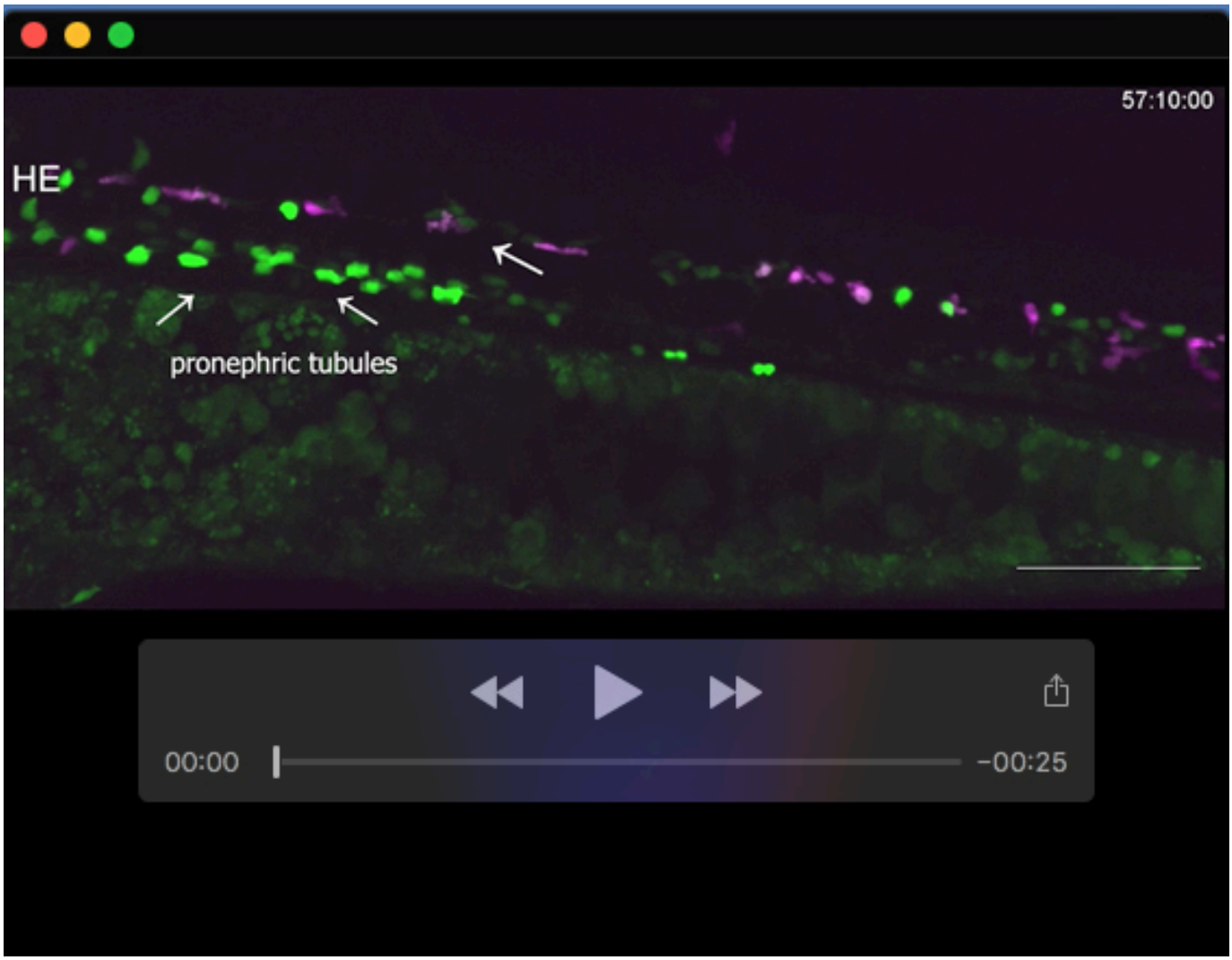

Movie 8. *lyz:DsRed2+/cd41:gfp+* cells in *vegfc* loss-of-function embryo late-stage DA.

Time-lapse imaging of *cd41:gfp* (HSPCs; green) and *lyz:DsRed2* (myeloid; magenta) *vegfc* loss-of-function embryos from 56-66 hpf. Arrows indicate *lyz:DsRed2+/cd41:gfp+* cells that reside in the DA and display crawling behavior. Corresponds to Figure 5F,G.

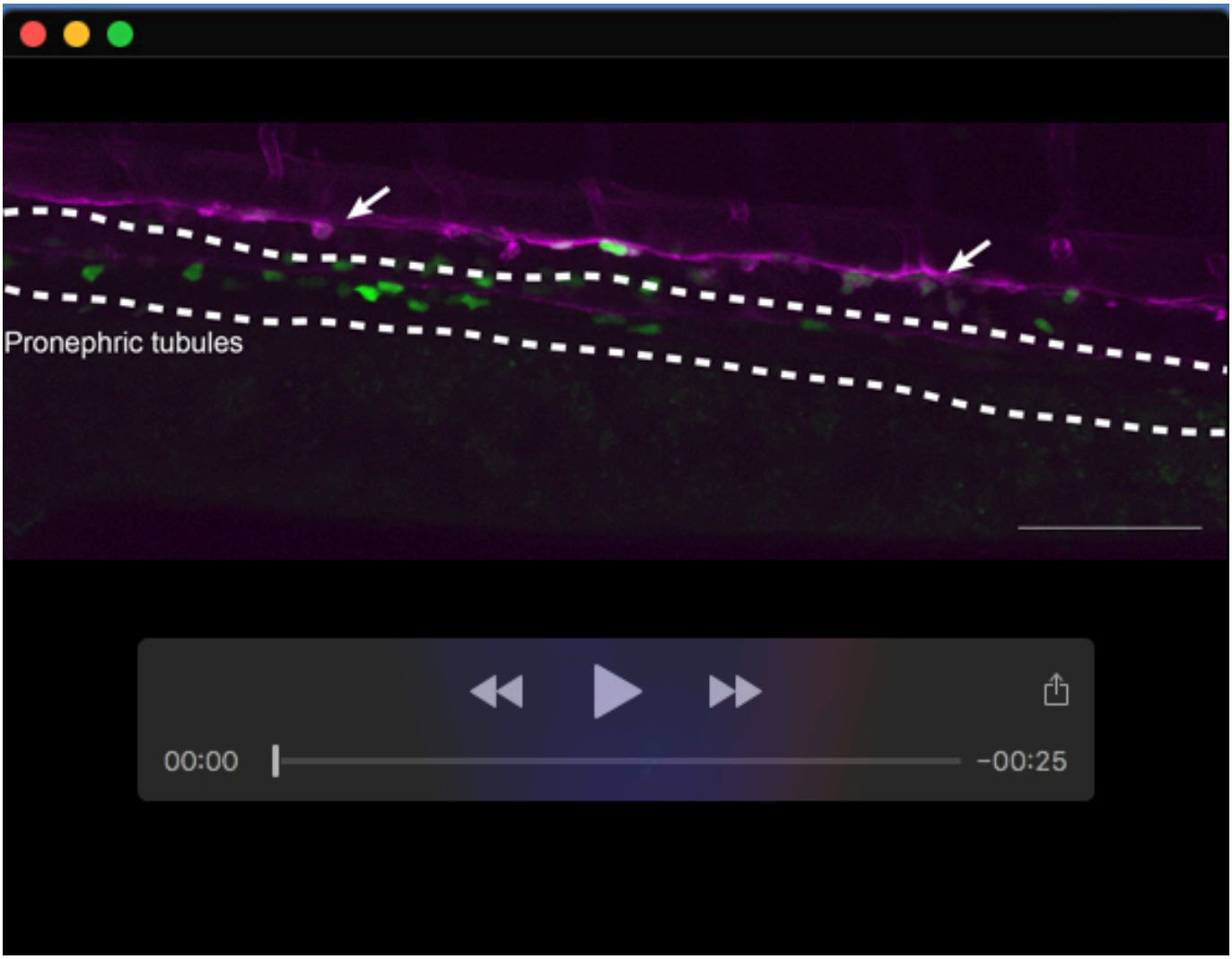

Movie 9. Vehicle treatment control (DMSO) and HSPC emergence from the DA.

Time-lapse imaging of *cd41:gfp* (HSPCs; green) and *flk:mCherry* (ECs; magenta) DMSO-treated control embryos from 48-52 hpf. Arrows indicate cells in the DA that are undergoing EHT. Corresponds to Figure 6B (DMSO).

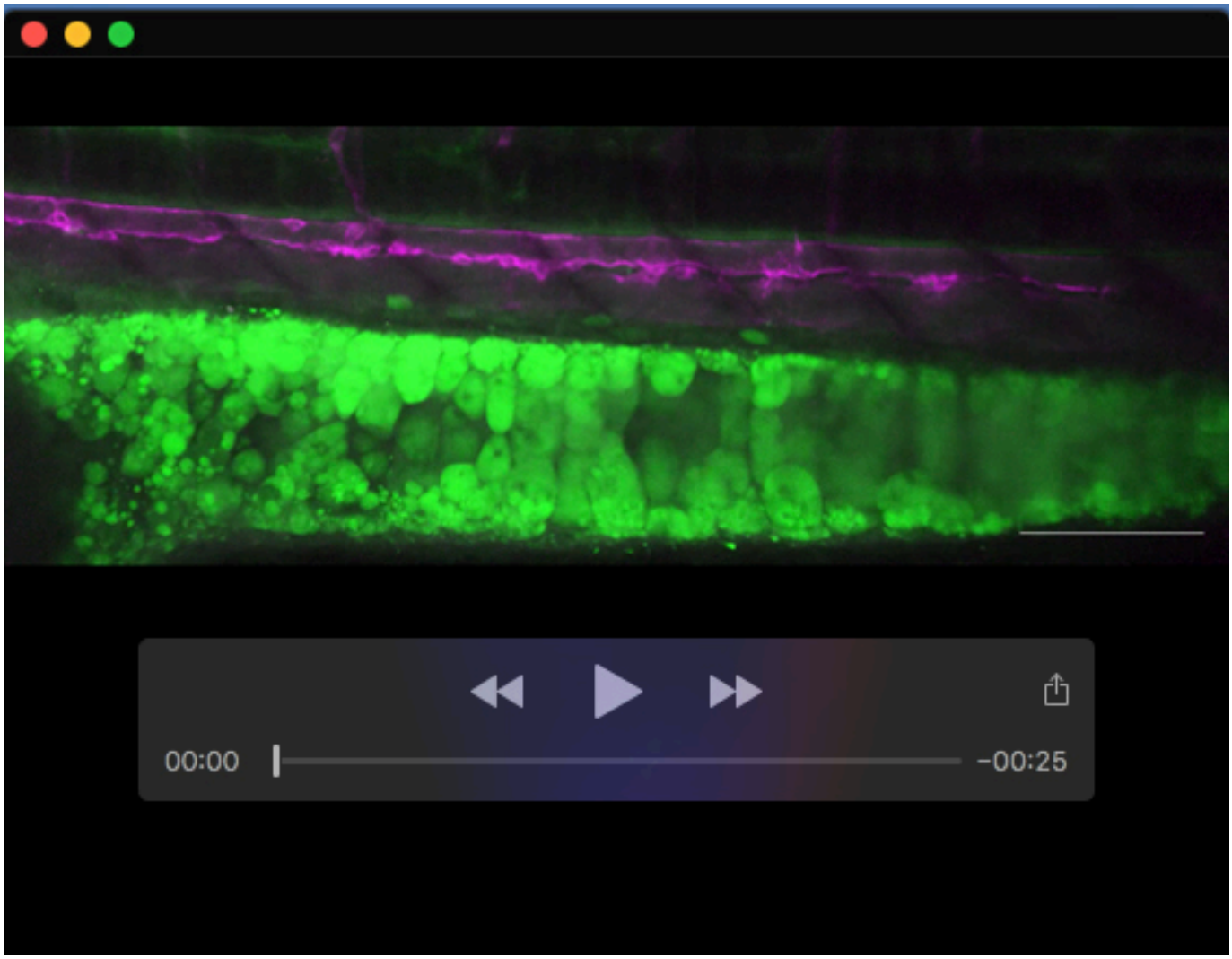

Movie 10. Vegf receptor inhibitor (SU5416) treatment and HSPC emergence from the DA.
Time-lapse imaging of *cd41:gfp* (HSPCs; green) and *flk:mCherry* (ECs; magenta) SU5416-treated embryos from 48-52 hpf. In this movie there are no obvious DA cells that complete EHT. Corresponds to Figure 6B (SU5416).

Supplementary References

BURGER, A., LINDSAY, H., FELKER, A., HESS, C., ANDERS, C., CHIAVACCI, E., ZAUGG, J., WEBER, L. M., CATENA, R., JINEK, M., ROBINSON, M. D. & MOSIMANN, C. 2016. Maximizing mutagenesis with solubilized CRISPR-Cas9 ribonucleoprotein complexes. *Development (Cambridge, England),* 143**,** 2025-2037.

CLEMENT, K., REES, H., CANVER, M. C., GEHRKE, J. M., FAROUNI, R., HSU, J. Y., COLE, M. A., LIU, D. R., JOUNG, J. K., BAUER, D. E. & PINELLO, L. 2019. CRISPResso2 provides accurate and rapid genome editing sequence analysis. *Nat Biotechnol,* 37**,** 224-226.

GAZIT, R., GARRISON, B. S., RAO, T. N., SHAY, T., COSTELLO, J., ERICSON, J., KIM, F., COLLINS, J. J., REGEV, A., WAGERS, A. J., ROSSI, D. J. & IMMUNOLOGICAL GENOME PROJECT, C. 2013. Transcriptome analysis identifies regulators of hematopoietic stem and progenitor cells. *Stem Cell Reports,* 1**,** 266-80.

SEITA, J., SAHOO, D., ROSSI, D. J., BHATTACHARYA, D., SERWOLD, T., INLAY, M. A., EHRLICH, L. I., FATHMAN, J. W., DILL, D. L. & WEISSMAN, I. L. 2012. Gene Expression Commons: an open platform for absolute gene expression profiling. *PLoS One,* 7**,** e40321.

ZHU, Q., GAO, P., TOBER, J., BENNETT, L., CHEN, C., UZUN, Y., LI, Y., HOWELL, E. D., MUMAU, M., YU, W., HE, B., SPECK, N. A. & TAN, K. 2020. Developmental trajectory of prehematopoietic stem cell formation from endothelium. *Blood,* 136**,** 845-856.